The 2011-2012 unrest at Santorini rift: Stress interaction between active faulting and volcanism

Nathalie Feuillet

The 2011–2012 unrest at Santorini rift: Stress interaction between active faulting and volcanism

Nathalie Feuillet[1]

Received 18 March 2013; revised 24 April 2013; accepted 27 April 2013; published 19 July 2013.

[1] At Santorini, active normal faulting controls the emission of volcanic products. Such geometry has implication on seismic activity around the plumbing system during unrest. Static Coulomb stress changes induced by the 2011–2012 inflation within a preexisting NW-SE extensional regional stress field, compatible with fault geometry, increased by more than 0.5 MPa in an ellipsoid-shaped zone beneath the Minoan caldera where almost all earthquakes (96%) have occurred since beginning of unrest. Magmatic processes perturb the regional stress in the caldera where strike-slip rather than normal faulting along NE-SW striking planes are expected. The inflation may have also promoted more distant moderate earthquakes on neighboring faults as the $M > 5$ January 2012, south of Christiania. Santorini belongs to a set of en echelon NE-SW striking rifts (Milos, Nysiros) oblique to the Aegean arc that may have initiated in the Quaternary due to propagation of the North Anatolian fault into the Southern Aegean Sea. **Citation:** Feuillet, N. (2013), The 2011–2012 unrest at Santorini rift: Stress interaction between active faulting and volcanism, *Geophys. Res. Lett.*, *40*, 3532–3537, doi:10.1002/grl.50516.

1. Introduction

[2] The Santorini volcano is the most active in the Aegean arc (Figure 1). Since the famous catastrophic Minoan eruption, ~3600 years ago, the volcanic activity is concentrated within the caldera and leads to the formation of the Kameni islands in its middle [*Druitt et al*., 1999]. The last eruption occurred in 1950. Since January 2011, the volcano reawakened with a sharp increase of the seismic activity beneath the Kameni islands (Figures 2 and 3) and surface deformation that was interpreted by the inflation of a magmatic source [*Newman et al*., 2012; *Papoutsis et al*., 2013]. That the magmatic inflation might increase the seismic hazard near Santorini has motivated this study. Interactions between faults and volcanoes exist at all space and time scales: faults may control the emission of volcanic vents and volcanic processes influence fault kinematics [e.g., *Rubin and Pollard*, 1988; *Ellis and King*, 1991; *Feuillet et al*., 2010]. Earthquakes and eruptions may correlate in time and two-way mechanical coupling through stress transfer was appealed to explain this [e.g., *Nostro et al*., 1998; *Hill et al*., 2002; *Walter and Amelung*, 2007; *Feuillet et al*., 2011].

[3] The Santorini volcanic complex was struck by magnitude >7 regional earthquakes as in 1956 between Ios and Amorgos [*Papadopoulos and Pavlides*, 1992] and may be an ideal place to investigate the relationship between faults and volcanic processes. The tectonic context of the volcano is however poorly documented. This paper has two main goals: (1) document the active faulting (geometry, kinematics) near the Santorini volcano to better understand the tectonic context of the volcano at local and more regional scales, and (2) explain the distribution of the seismicity associated to the 2011–2012 inflation within this tectonic context.

[4] By using bathymetric and topographic data at several scales combined with seismological evidences, active faulting geometry and kinematics in the Santorini region are first assessed. Static Coulomb stress changes induced by the 2011–2012 unrest are then calculated within a stress regime compatible with fault geometry to explain the distribution of seismicity and the deformation style in the Minoan Caldera. Finally, active faulting and volcanism at Santorini are discussed within the regional Aegean sea seismotectonic frame.

2. Kinematics of Active Faulting in Santorini

[5] On the basis of recently published marine charts [*Nomikou et al*., 2012] and following an approach that consists in using bathymetry to constrain the geometry of finite tectonic strain on the oceanic floor [e.g., *Feuillet et al*., 2010], it was possible to map and characterize active faults that offset the seafloor around Santorini by using perturbations of bathymetric gradients. Steep gradients between slope breaks allow fault throws to be estimated from orthogonal profiles, and available seismic profiles reveal fault geometry at depth (see auxiliary material S1).

[6] The active fault map is presented in Figure 2. The bathymetry is simplified, but faults and other morphological features were mapped from the high-resolution map published by *Nomikou et al*. [2012]. The Santorini volcano is located in a 40 km-wide normal fault system that veers clockwise from N-E direction, to the East, to E-W, to the west of the volcano. The largest faults (Christiania, Anafi) bounding the system to the south are several tens of kilometer long, dip southwards, strike $N90 \pm 20°E$ and have scarps of several hundred meters high (~650 m for Anafi). North of these major structures, smaller NE-SW striking faults, with several tens to few hundred meters-high scarps, cut the seafloor near Santorini and form a second family. With a 200 m high scarp, the $N40 \pm 10°E$ striking, south dipping Ios fault is one of the largest of this system. West of Santorini, it

Additional supporting information may be found in the online version of this article.

[1]Institut de Physique du Globe de Paris, UMR 7154 CNRS, Sorbonne Paris Cité, Paris, France.

Corresponding author: N. Feuillet, Institut de Physique du Globe de Paris, Sorbonne Paris Cité, Univ Paris Diderot, UMR 7154 CNRS, 1 rue Jussieu, F-75238 Paris CEDEX 05, France. (feuillet@ipgp.fr)

0094-8276/13/10.1002/grl.50516

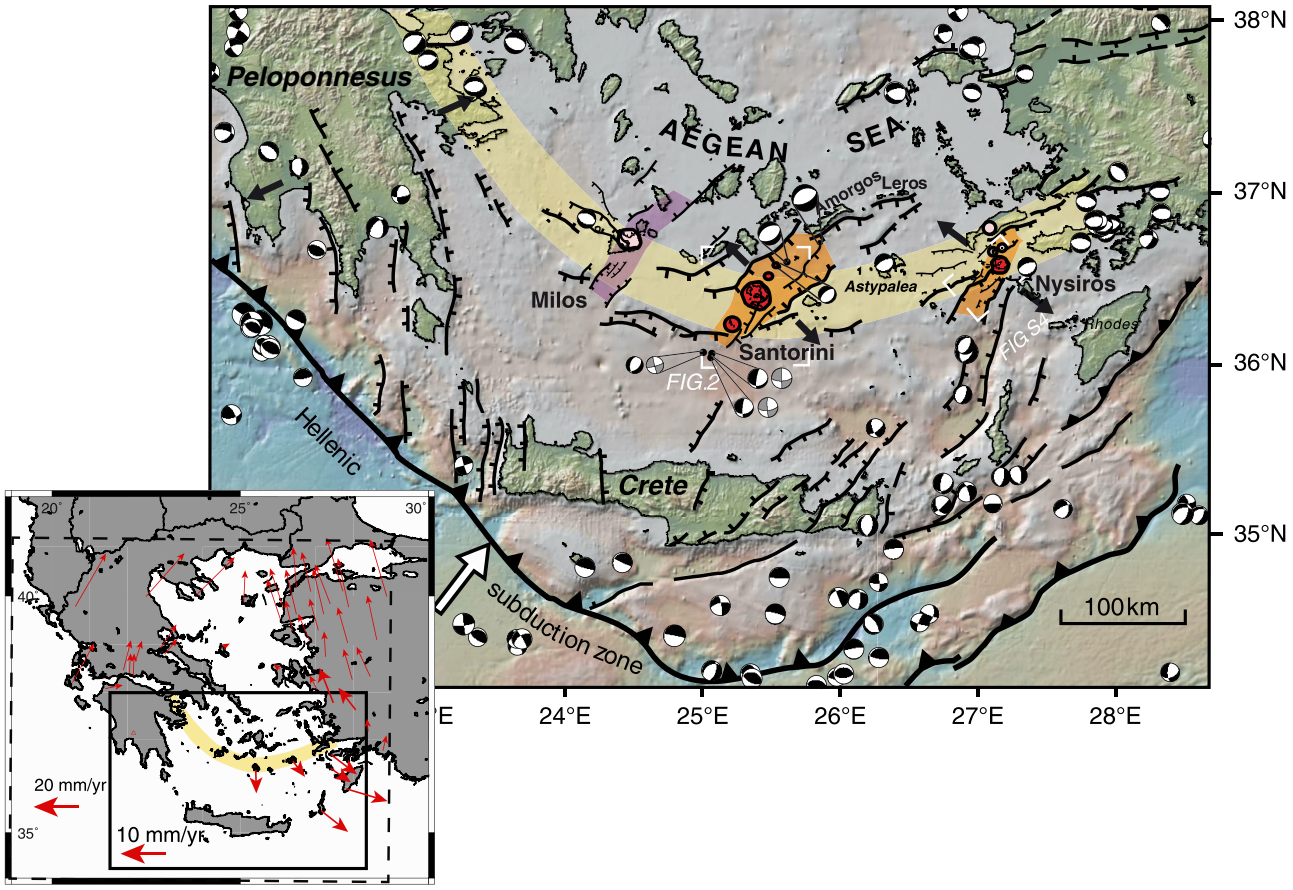

Figure 1. Seismotectonic map of Aegean. Bathymetry and topography from GeomapApp database (http://www.geomapapp.org). Main faults from *Armijo et al*. [1992, 1996], *Piper and Perissoratis* [2003], and *Nomikou and Papanikolaou* [2011] modified from this study by using bathymetric data published in the GeomapApp database, *Nomikou et al*. [2012], and *Brosolo et al*. [2012]. Focal mechanisms are from Harvard (http://www.globalcmt.org/CMTsearch.html), *Okal et al*. [2009], *Dimitriadis et al*. [2009], National Observatory of Athens (for the 26 June 2009 event), and *Kiratzi* [2013] (in gray). In orange and purple (less active): Milos, Santorini, and Nysiros rifts. Yellow band: Aegean arc. Red circle: active volcanic complex. Pink circles: no more or very little active volcanoes. White arrow: convergence between Africa and Aegean [e.g., *Reilinger et al*., 2010]. Locations of Figure 2 and S4 (auxiliary material S4) are indicated. Inset: in dashed box, GPS vectors of *Reilinger et al*. [2010] in red with western Aegean fixed. Black box: location of Figure 1.

veers to a more E-W direction and connects to the N90 to N130°E striking, southwards dipping Sikinos fault zone. Northeast of Santorini, it composes, with the northwards dipping N45°E striking Santorini-Amorgos ridge faults, the Anydhros graben. The 500 m deep Santorini-Anafi valley is also a NE-SW striking graben bounded by two antithetic normal fault systems: the northward dipping faults of Santorini-Anafi system, which scarps are up to 200 m high, and the south-dipping faults bounding the Santorini-Amorgos ridge to the south. The graben guides the emplacement of large-scale debris avalanche deposits. Southwest of Santorini, numerous N30 ± 10°E striking faults, cut across the more E-W striking faults (Christiana) suggesting that the former postdates the latter. These faults belong to the Christiana fault zone and structure the Christiana-Santorini horst. One of them, dipping to the northwest, encroaches the Santorini island bounding to the north the pre-volcanic basement.

[7] The Santorini volcano belongs to a large volcanic complex formed by several vents (Christinia, Santorini-Kameni, Kolumbo) aligned in a ~N40°E direction [*Vougioukalakis and Fytikas*, 2005], parallel to the NE-SW striking faults. As Santorini, the submarine Kolumbo volcano is active and last erupted in 1650 AD, killing 70 people in Santorini and promoting a damaging tsunami [*Dominey-Howes et al*., 2000]. The Kolumbo volcano aligns with 19 others volcanic domes [*Nomikou et al*., 2012] parallel to faults, within the Anydhos graben floor, probably along fissures accommodating the NW-SE extension between the bounding faults (Figure 2).

[8] As observed elsewhere in magma-rich extensional environment, volcanic complexes tend to emplace along fissures perpendicular to the minimum compressive stress σ3 [*Anderson*, 1938]. Both the arrangement of volcanic vents and the pattern of recent faulting are compatible with a NW-SE local extension at Santorini. Overall, faults and volcanoes structure a NE-SW striking rift.

[9] Two moderate earthquakes of magnitude larger than 5 occurred on 26 and 27 January 2012 south of the Christiana fault and were followed by numerous aftershocks (Figure 3). The focal mechanisms of the main shock and the two main aftershocks indicate that these events may have ruptured

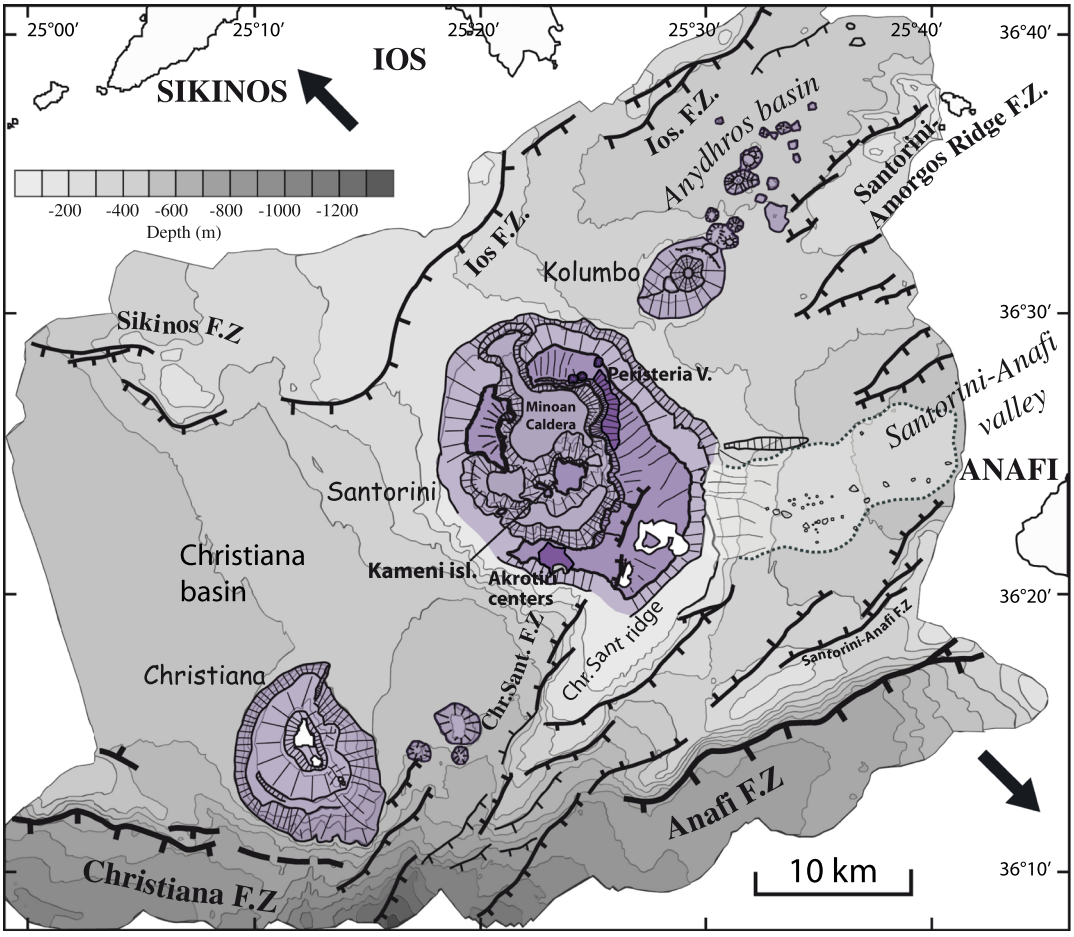

Figure 2. Active faulting around the Santorini volcanic complex. Bathymetric chart redrawn from *Nomikou et al*. [2012] with 100 m interval. No data in white areas. Fault in black, with thicker traces for higher scarps. Arrows: local direction of extension. In purple: Santorini complex with darker areas, older volcanic centers. In white on Santorini: old pre-volcanic basement. F. Z.: Fault zone. Dashed line delineates debris avalanche deposits with a characteristic hummocky morphology very clear in the bathymetry [*Croff Bell et al*., 2012].

NNE-SSW to NE-SW-striking normal or N-S strike-slip faults [*Kiratzi*, 2013] prolonging the Christiana-Santorini system towards the south and accommodating a NW-SE extension.

[10] The focal mechanisms calculated for the larger two $M > 7$ earthquakes on 9 August 1956 are also compatible with such an extension. At a larger scale, the Ios fault system prolongs to the NE towards Amorgos and is relayed by other south-dipping normal faults that bound to the south the insular shelves of Amorgos and Leros (Figure 1). The 1956 earthquake may have ruptured the entire 70 km long Ios fault in agreement with the rupture size proposed by *Okal et al*. [2009], distribution of aftershocks and isoseismal maps [*Papadopoulos and Pavlides*, 1992]. With a magnitude equal to and maybe larger than 7.5, the main shock of the 9 August 1956 was the largest one to strike Greece in the twentieth century [*Okal et al*., 2009]. Given the moderate seismic activity in the area and the rarity of earthquakes of this size, it is noteworthy that the 1950 Santorini eruption occurred only 6 years before the 1956 earthquake.

[11] Today, most of the instrumental seismicity concentrates in the Ios fault hanging wall, mainly around the Kolumbo volcanic system. Several events have focal mechanisms also compatible with a NW-SE extension and faulting geometry [*Dimitriadis et al*., 2009] as the Magnitude 4.6, 26 June 2009 event (Figures 1 and 3).

3. Coulomb Stress Induced by the 2011–2012 Unrest in Santorini

[12] *Newman et al*. [2012] show that the surface deformations measured by Global Positioning System (GPS) since the beginning of the Santorini unrest can be modeled by an inflation of 14 million m^3 of a magmatic spherical body located at 4 km depth beneath the caldera. Following a strategy fully described and discussed in *Feuillet et al*. [2004], we calculated the Coulomb stress changes induced by this inflation in a local NW-SE striking extensional stress regime compatible with fault kinematics at Santorini. The effects of changing all modeling parameters (regional stress orientation and magnitude, Lamé's coefficients values, and source parameters) were tested and are discussed in the auxiliary material S2.

[13] The Coulomb stress changes are calculated on planes optimally oriented for Coulomb failure (OOPs) by using the equation:′

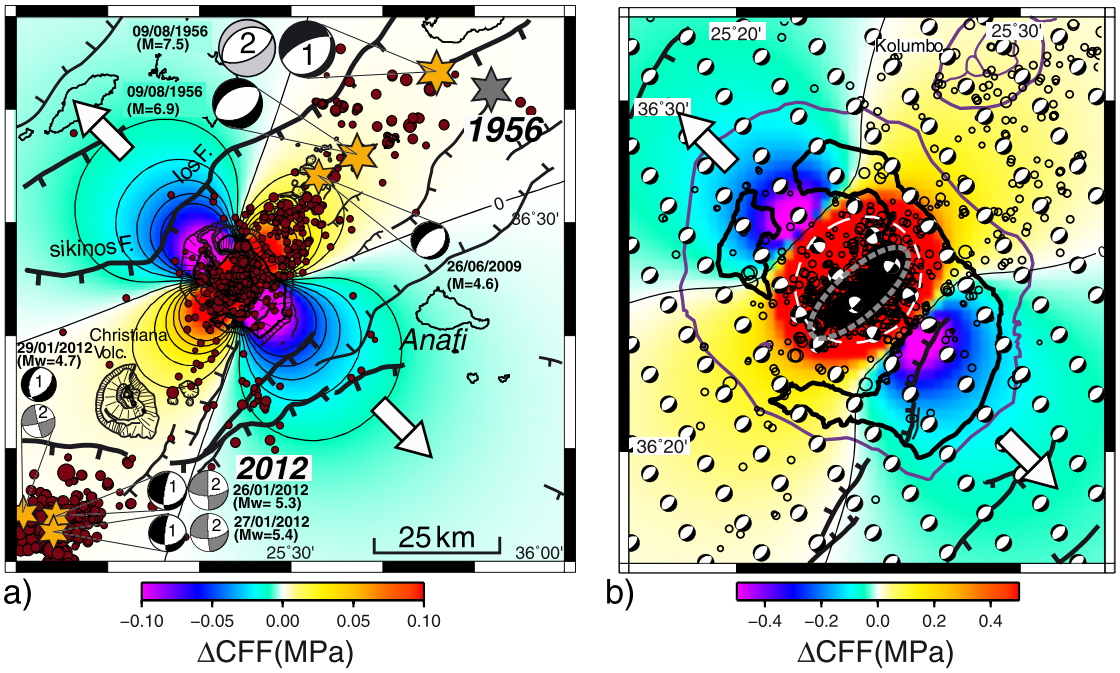

Figure 3. Static coulomb stress changes induced by the 2011–2012 magmatic inflation at Santorini in an extensional stress regime (White double arrows). See text for modeling parameters. Seismicity from Geophysical lab. Auth. and available on http://www.volcanodiscovery.com/santorini/seismic-activity-2011.html between 09/2011 and 05/2012 plus seismicity recorded between 01/2011 and 01/2012 in the Caldera [*Newman et al*., 2012]. Most earthquakes have magnitude less than 3.0 in the Santorini rift. Larger events ($M > 5$) however occurred in January 2012 south of Christinia. (a) Coulomb stress changes in the Santorini rift. Orange and gray stars: Large and moderate magnitude earthquakes of 1956 and 2012. Gray star: Epicenter of the 1956 mainshock from *Dimitriadis et al*. [2009]. Faults as in Figure 2 (but simplified). Focal mechanisms as in Figure 1. The 1956 mainshock focal mechanism number 1 is from *Okal et al*. [2009] and number 2, from, e.g., *Dimitriadis et al*. [2009]. The 2012 earthquake focal mechanisms is in gray from *Kiratzi* [2013]. Contour interval: 0.01 MPa between −0.05 and 0.05 MPa. (b) As in Figure 3a but at larger scale with predicted focal mechanisms on the left lateral optimally oriented planes (OOPs) for rupture. Faults as in Figure 2. White dashed line: area of Coulomb stress increase >2 MPa. Gray dashed area: area where the seismic swarm is much denser.

$$\Delta CFF = \Delta\tau + \mu'\Delta\sigma_n$$

where $\Delta\tau$ is the shear stress change computed in the direction of slip on the faults, $\Delta\sigma_n$ is the normal stress change (positive for extension), and μ' is the effective coefficient of friction [*Harris*, 1998; *King and Cocco*, 2001]. The OOPs are determined from the total stress: regional stress field plus induced stress perturbation caused by the unrest. Two conjugate planes are optimally oriented for stress, the Coulomb stress changes being identical on both planes and the focal mechanism is associated to each plane.

[14] Dike opening (closing) or pressure changes are modeled as planar dislocations in an elastic homogeneous half-space [*Okada*, 1992]. Opening of three orthogonal dikes, intersecting in their center, simulates the expansion of a spherical magma chamber see discussion in S2). All parameters are listed in Table 1.

Table 1. Model Parameters

Lon (°)	Lat (°)	Depth	Length (m)	Width (m)	Opening (m)	ΔV^a $10^6 m^3$	Strike, Dip, Rake
25.405[a]	36.415[a]	4.0[a]	200	200	210	8.4	0, 90, 90
25.405[a]	36.415[a]	4.0[a]	200	200	210	8.4	90, 90, 90
25.405[a]	36.415[a]	4.0[a]	200	200	210	8.4	0, 0, 90

[a]Location from *Newman et al*. [2012], within 95% confidence region.

[15] The regional stress is extensional with a σ3 axis subhorizontal and oriented 135°E and a vertical σ1 axis. I considered here a deviatoric regional stress tensor; the magnitude of the regional stress is set to 3 MPa, equivalent to the stress drop of 3.3 estimated for the 1956 Earthquake [*Okal et al*., 2009]. All calculations were made in an elastic half space with a conventional value of 32 GPa for λ and μ.

[16] I used the constant apparent friction model with $\mu' = 0.4$, equivalent to laboratory value of friction and modest fluid pressure. In volcanic area, however, the presence of fluids can contribute to alter the fault friction and may strongly affect the Coulomb stress changes. I thus examine also the effect of using an isotropic poroelastic model instead of constant apparent friction model (see auxiliary material S2).

[17] The modeling results are presented in Figure 3 in map view at 3 km depth (mid-depth of earthquake hypocenters in the Santorini Caldera, between 1 and 6 km, *Newman et al*., [2012]). The Coulomb stress increased by more than 0.5 MPa within an ellipsoid elongated perpendicular to the minimum compressive stress direction beneath the Minoan Caldera and Kameni islands. A total of 96% of the earthquakes recorded at Santorini island occurred in an area of Coulomb stress increase, 83% in an area where the stress has increased by more than 0.5 MPa, and 80% in an area where the stress increased

by more than 2 MPa. Outside this area, the Coulomb stress has decreased by more than 0.5 MPa within two lobes oriented along the extension direction explaining why only very few earthquakes occurred in this area since the beginning of the unrest. The denser seismic swarm (dotted gray line in Figure 3) is elongated and parallel to the ellipsoid major axis indicating that the preexisting extensional stress plays an important role in the unrest-induced seismicity distribution. The seismicity pattern is well explained by modeling the stress changes with a strong regional stress magnitude of 10 MPa (see auxiliary material Figure S2h).

[18] The inflation has contributed to perturb the regional extensional stress field in the caldera. Far from the influence of the volcanic source, the focal mechanisms predicted by Coulomb failure are compatible with the regional stress field with normal faulting on NE striking nodal planes. Near the volcanic source, predicted focal mechanisms are heterogeneous and show strike-slip motion on vertical faults oriented in a radial way around the volcanic source.

[19] At larger scale, the volcanic processes affect the whole Santorini complex between Kolumbo and Christiana (Figure 3a). South of Christiana, where the 26 and 27 January 2012 M5+ earthquakes occurred, the Coulomb stress, either calculated on OOPs in a preexisting regional stress or on the 26 January 2012 mainshock focal mechanism nodal planes (see auxiliary material S3), is very slightly increased (<0.01 MPa). These small values are however much larger than the stress changes induced by ocean or solid-earth tides that may be sufficient to trigger earthquakes and volcanic activity [*Kasahara*, 2002; *Métivier et al*., 2009]. Earthquakes of that magnitude are rare in the area; and given the temporal coincidence of events, the magmatic inflation may have promoted the January 2012 earthquakes. The 2011 inflation has also increased the Coulomb stress along other neighboring faults and may have brought them closer to failure, thus increasing the seismic hazard in the area.

[20] The 1956 earthquake epicenters are located in an area of stress increase. If the 1950 volcanic unrest was also associated with inflation of a magmatic chamber beneath the caldera, it may have promoted the 1956 $M > 7$ earthquake few years later.

4. The Santorini Rift in the Framework of Aegean Sea Active Deformation

[21] The Santorini volcano lies in a NE-SW striking rift resulting from a NW-SE striking extension, compatible with fault geometry, alignments of volcanic vents, focal mechanisms of earthquakes, and GPS data. This tectonic regime affects all quaternary volcanic complex of the central Aegean arc. New bathymetric data [*Nomikou and Papanikolaou*, 2011] reveal that the young 160 kyr old [*Vougioukalakis and Fytikas*, 2005] Nysiros volcanic complex is developing at the northeastern tip of a large NE-SW striking graben structuring the Nysiros basin and accommodating a NW-SE extension (see detailed tectonic map in auxiliary material S4). The central part of the volcano is composed by a set of volcanic vents aligned parallel to faults and probably emplaced along fissures opened inside the rift floor.

[22] *Piper and Perissoratis* [2003] have shown, on the basis of seismic reflection profiles, that numerous NNE-SSW to NE-SW striking Quaternary active normal faults crosscut the seafloor around Milos. These faults prolong onshore and structure a graben in which the most recent Pleistocene to present volcanic products have emplaced, among them the 500 to 90 ka old Fyriplaka Volcano [*Stewart and McPhie*, 2006]. The Milos rift is however much less active than Nysiros and Santorini with a lower rate of seismicity [*Bohnoff et al*., 2006] and no magmatic eruption during the Holocene [*Principe et al*., 2003]. Overall, this is compatible with much lower deformation rates measured by GPS at this place.

[23] Milos, Santorini, and Nysiros rifts are oblique to the Aegean arc, parallel to the convergence along the Hellenic trench and arranged in sinistral echelons (Figure 1). These rifts crosscut or connect, in an oblique manner, an older normal fault system, parallel to the arc that may be now less active. These older faults have opened in the Late Cenozoic due to the back-arc extension [*Armijo et al*., 1996]. Seismic and core data as well as microtectonic measurements have revealed a very recent transition (less than 1 Ma) between the N-S extension to a NW-SE extension along the central part of the Aegean Sea [*Piper and Perissoratis*, 2003; *Mercier et al*., 1989]. The NE-SW rift bounding faults may have initiated at this time. *Piper and Perissoratis* [2003] showed that age of faulting decreases eastwards, with the age of volcanic complexes, along the arc, from Milos to Nysiros, from 0.8 to 0.2 Ma. This suggests that rifting has propagated eastwards through time.

[24] GPS data [*Reilinger et al*., 2010] show that the southeastern part of the Aegean moves southeastwards compare to the western part (Figure 1). Rift opening may accommodate this motion increasing, toward the eastern Hellenic trench, from 5 (in Astypalea) to 10 mm/yr (in Rhodes). The Santorini-Anafi valley subsides at rate of 2.5 mm/yr since 200 ka [*Piper and Perissoratis*, 2003]. Considering graben-bounding fault dips ranging between 40 and 80°, this implies extension rates of 3 ± 2 mm/yr comparable to GPS measurements in Santorini and Astypalea.

[25] Initiation of rifting along the eastern part of Aegean arc is contemporaneous with the opening of the Corinth Rift and the propagation of the North Anatolian fault (NAF) into the southern Aegean [*Armijo et al*., 1996]. It postdates others N-S striking faults in Southern Peloponnesus and Crete (2–4 Ma, *Armijo et al*., [1992]) originating from incipient collision of the Hellenic arc with the buoyant African Margin [*Lyon-Caen et al*., 1988; *Ganas and Parson*, 2009]. Milos, Santorini, and Nysiros rifts may result from the southeastwards motion of the SE Aegean Sea promoted, in mid-late Quaternary, by the propagation of the NAF into the southern Aegean Sea, in a collisional context at the Hellenic trench southern boundary.

5. Conclusions

[26] The Santorini volcano emplaced with other vents (Kolumbo, Christiani) within, and parallel to, a mid-late Quaternary active NE-SW normal fault system composing a rift oblique to the Aegean arc. The rift connects to or crosscuts older E-W striking faults resulting from back-arc extension in early Pliocene. This particular geometry implies that faults control the emission of volcanic products in the central and eastern Aegean arc. Link between active faulting and

volcanism is well illustrated by the ongoing volcanic unrest at Santorini. The volcano is developing in a NW-SE extensional stress field that controls the distribution of seismic activity promoted by the volcanic unrests. By calculating the Coulomb stress changes induced by the 2011–2012 magmatic inflation within a preexisting NW-SE extensional stress field compatible with mid-late Quaternary fault geometry, I showed that the Coulomb stress has increased in the Caldera within an ellipsoid-shaped area elongated perpendicularly to the minimum compressive stress. A total of 96% of the earthquakes have occurred in this area suggesting that the seismicity was triggered by the Coulomb stress increase. The pattern of the Coulomb stress increase mimics that of seismic swarm indicating that the regional stress may be quite strong and plays probably an important role in the seismicity distribution. Larger regional earthquakes may also have occurred along the Santorini normal fault system as in 1956 and 2012. Some may have been triggered by volcanic processes. Milos and Nysiros are also located in arc oblique rifts. Quaternary rifting in central and eastern Aegean arc may accommodate the southeastward motion of the southeastern Aegean Sea promoted by the southward propagation of the NAF into the Aegean Sea.

[27] **Acknowledgments.** I thank Claude Jaupart for encouraging this work. It has benefited from numerous discussions with Rolando Armijo and Robin Lacassin. I am grateful to M. E. Belardinelli, G. A. Papadopoulos, A. Ganas, and an anonymous reviewer for constructive reviews. This is IPGP contribution 3398.

[28] The Editor thanks Gerassimos A. Papadopoulos and Athanassios Ganas for their assistance in evaluating this paper.

References

Anderson, E. M. (1938), The dynamics of sheet intrusion, *Proc. R. Soc. Edinb.*, *58*, 242–251.

Armijo, R., H. Lyon-Caen, and D. Papanastassiou (1992), East–west extension and Holocene normal-fault scarps in the Hellenic arc, *Geology*, *20*, 491–494.

Armijo, R., B. Meyer, G. C. P. King, A. Rigo, and D. Papanastassiou (1996), Quaternary evolution of the Corinth rift and its implications for the Late Cenozoic evolution of the Aegean, *Geophys. J. Int.*, *126*, 11–53.

Bohnhoff, M., M. Rische, T. Meier, D. Becker, G. Stavrakakis, and H. P. Harjes (2006), Microseismic activity in the Hellenic Volcanic Arc, Greece, with emphasis on the seismotectonic setting of the Santorini–Amorgos zone, *Tectonophysics*, *423*, 17–33.

Brosolo, L., J. Mascle, and B. Loubrieu (2012), *Morpho-Bathymetry of the Mediterranean Sea*, First edition, Publication CGMW/UNESCO, Scale: 1/4000000, Paris.

Croff Bell, K. L., S. N. Carey, P. Nomikou, H. Sigurdsson, and D. Sakellariou (2012), Submarine evidence of a debris avalanche deposit on the eastern slope of Santorini volcano, Greece, doi:org/10.1016/j.tecto.2012.05.006.

Dimitriadis, I., E. Karagianni, D. Panagiotopoulos, C. Papazachos, P. Hatzidimitriou, M. Bohnhoff, M. Rische, and T. Meier (2009), Seismicity and active tectonics at Kolumbo Reef (Aegean Sea, Greece): Monitoring an active volcano at Santorini Volcanic Center using a temporary seismic network, *Tectonophysics*, *465*, 136–149.

Dominey-Howes, D. T. M., G. A. Papadopoulos, and A. G. Dawson (2000), Geological and historical investigation of the 1650 Mt. Columbo (Thera Island) eruption and tsunami, Aegean Sea, Greece, *Nat. Hazards*, *21*(1), 83–96.

Druitt, T. H., L. Edwards, R. M. Mellors, D. M. Pyle, R. S. J. Sparks, M. Lanphere, M. Davies, and B. Barriero (1999), Santorini Volcano, *Geol. Soc. London Mem.*, *19*, 165.

Ellis, M., and G. King (1991), Structural control of flank volcanism in continental rifts, *Science*, *254*, 839–842.

Feuillet, N., C. Nostro, C. Chiarabba, and M. Cocco (2004), Coupling between earthquake swarms and volcanic unrest at the Alban Hills Volcano (central Italy) modeled through elastic stress transfer, *J. Geophys. Res.*, *109*, B02308, doi:10.1029/2003JB002419.

Feuillet, N., et al. (2010), Active faulting induced by slip partitioning in Montserrat and link with volcanic activity: New insights from the 2009 GWADASEIS marine cruise data, *Geophys. Res. Lett.*, *37*, L00E15, doi:10.1029/2010GL042556.

Feuillet, N., F. Beauducel, and P. Tapponnier (2011), Tectonic context of moderate to large historical earthquakes in the Lesser Antilles and mechanical coupling with volcanoes, *J. Geophys. Res.*, *116*, B10308, doi:10.1029/2011JB008443.

Ganas, A., and T. Parsons (2009), Three-dimensional model of Hellenic Arc deformation and origin of the Cretan uplift, *J. Geophys. Res.*, *114*, B06404, doi:10.1029/2008JB005599.

Harris, R. A. (1998), Introduction to special session: Stress triggers, stress shadows, and implications for seismic hazard, *J. Geophys. Res.*, *103*, 24,347–24,358.

Hill, D. P., F. Pollitz, and C. Newhall (2002), Earthquake-volcano interactions, *Phys. Today*, *55*, 41–47, doi:10.1063/1.1535006.

Kasahara, J. (2002), Tides, earthquakes, and volcanoes, *Science*, *297*, 348.

King, G. C. P., and M. Cocco (2001), Fault interaction by elastic stress changes: New clues from earthquake sequences, *Adv. Geophys.*, *44*, 1–38.

Kiratzi, A. (2013), The January 2012 earthquake sequence in the Cretan Basin, south of the Hellenic Volcanic Arc: Focal mechanisms, rupture directivity and slip models, *Tectonophysics*, *586*, 160–172.

Lyon-Caen, H. et al. (1988), The 1986 Kalamata (South Peloponnesus) earthquake: Detailed study of a normal fault, evidences for east–west extension in the Hellenic arc, *J. Geophys. Res.*, *93*, 14,967–15,000.

Mercier, J. L., D. Sorel, P. Vergely, and K. Simeakis (1989), Extensional tectonic regimes in the Aegean basins during the Cenozoic, *Basin Res.*, *2*, 49–71.

Métivier, L., O. De Viron, C. P. Conrad, S. Renault, M. Diament, and G. Patau (2009), Evidence of earthquake triggering by the solid earth tides, *Earth. Planet. Sci. Lett.*, *278*, 370–375.

Newman, A. V., et al. (2012), Recent geodetic unrest at Santorini Caldera, Greece, *Geophys. Res. Lett.*, *39*, L06309, doi:10.1029/2012GL051286.

Nomikou, P., and D. Papanikolaou (2011), Extension of active fault zones on Nisyros volcano across the Yali-Nisyros channel based on onshore and offshore data, *Mar. Geophys. Res.*, *32*, 181–192, doi:10.1007/s11001-011-9119.

Nomikou, P., S. Carey, D. Papanikolaou, K. L. C. Bell, D. Sakellariou, M. Alexandri, and K. Bejelou (2012), Submarine Volcanoes of the Kolumbo volcanic zone NE of Santorini Caldera, Greece, *Glob. Planet. Change*, doi:10.1016/j.gloplacha.2012.01.001.

Nostro, C., R. S. Stein, M. Cocco, M. E. Belardinelli, and W. Marzocchi (1998), Two-way coupling between Vesuvius eruptions and southern Apennine earthquakes, Italy, by elastic stress transfer, *J. Geophys. Res.*, *103*, 24,487–24,504.

Okada, Y. (1992), Internal deformation due to shear and tensile faults in a half-space, *Bull. Seismol. Soc. Am.*, *82*, 1018–1040.

Okal, E. A., C. E. Synolakis, B. Uslu, N. Kalligeris, and E. Voukouvalas (2009), The 1956 earthquake and tsunami in Amorgos, Greece, *Geophys. J. Int.*, *178*, 1533–1554.

Papadopoulos, G. A., and S. B. Pavlides (1992), The large 1956 earthquake in the South Aegean: Macroseismic field configuration, faulting, and neotectonics of Amorgos island, *Earth. Planet. Sci. Lett.*, *113*, 383–396.

Papoutsis, I., X. Papanikolaou, M. Floyd, K. H. Ji, C. Kontoes, D. Paradissis, and V. Zacharis (2013), Mapping inflation at Santorini volcano, Greece, using GPS and InSAR, *Geophys. Res. Lett.*, *40*, 267–272, doi:10.1029/2012GL054137.

Piper, D. J. W., and C. Perissoratis (2003), Quaternary neotectonics of the South Aegean arc, *Mar. Geol.*, *198*, 259–288.

Principe, C., Arias, A. and U. Zoppi (2003). Hydrothermal explosions on Milos: From debris avalanches to debris flows deposits, In "The South Aegean Active Volcanic Arc: Present Knowledge and Future Perspectives" international conference, Milos 2003. Book of abstracts 95.

Reilinger, R., S. McClusky, D. Paradissis, S. Ergintav, and P. Vernant (2010), Geodetic constraints on the tectonic evolution of the Aegean region and strain accumulation along the Hellenic subduction zone, *Tectonophysics*, *488*, 22–30.

Rubin, A. M., and D. D. Pollard (1988), Dike-induced faulting in rift zones of Iceland and Afar, *Geology*, *16*, 413–417.

Stewart, A. L., and J. Mc Phie (2006), Facies architecture and Late Pliocene – Pleistocene evolution of a felsic volcanic island, Milos, Greece, *Bull. Volcanol.*, *68*, 703–726, doi:10.1007/s00445-005-0045-2.

Vougioukalakis, G. E., and M. Fytikas (2005), M. Volcanic hazards in the Aegean area, relative risk evaluation, monitoring and present state of the active volcanic centers, The South Aegean Active Volcanic Arc, Edited by M.Fytikas and G.E. Vougioukalakis, *Dev. Volcanol.*, *7*, 161–183.

Walter, T. R., and F. Amelung (2007), Volcanic eruptions following $M \geq 9$ megathrust earthquakes: Implications for the Sumatra Andaman volcanoes, *Geology*, *35*(6), 539–542.